The Soil Moisture Active Passive (SMAP) Radar: Measurements at High Latitudes and of Surface Freeze/Thaw State

Michael Spencer, Scott Dunbar, Curtis Chen
Jet Propulsion Laboratory, California Institute of Technology

***Abstract*- The Soil Moisture Active/Passive (SMAP) mission is scheduled for a late 2014 launch date. The mission will use both active radar and passive radiometer instruments at L-Band in order to achieve the science objectives of measuring soil moisture and land surface freeze-thaw state. To achieve requirements for a wide swath at sufficiently high resolution for both active and passive channels, an instrument architecture that uses a large rotating reflector is employed. In this paper, focus will be placed on the radar design. The radar will employ synthetic-aperture processing to achieve a "moderate" resolution dual-pol product over a 1000 km swath. Because the radar is operating continuously, very frequent temporal coverage will be achieved at high latitudes. This data will be used to produce a surface freeze/thaw state data product.**

I. INTRODUCTION

The science objectives of SMAP are to provide frequent, global measurements of surface soil moisture and surface freeze/thaw state. These measurements will be used to enhance the understanding of water, energy, and carbon cycles, as well as improve weather and climate prediction. To measure both soil moisture and freeze/thaw state at the required resolution, a combined active/passive L-Band microwave instrument is employed [1]. The key instrument requirements were determined to be: 1) Dual-polarization L-Band radiometer measurements at 40 km resolution, 2) Linear HH, VV and HV (or VH) L-Band radar measurements at 3 km resolution or better, and 3) A wide swath to ensure global three-day refresh time for these measurements (1000 km swath at the selected equatorial orbital altitude of 685 km).

Previous publications have provided high-level descriptions of the SMAP instrument [2]. To accomplish the challenging set of requirements, a 6-meter, conically-scanning reflector antenna architecture was selected for the instrument design. The deployable mesh antenna is shared by both the radiometer and radar instruments by using a single L-Band feed. (An artist rendition of the mesh antenna, rotating spot beam, and associated wide swath is shown in Fig. 1.)

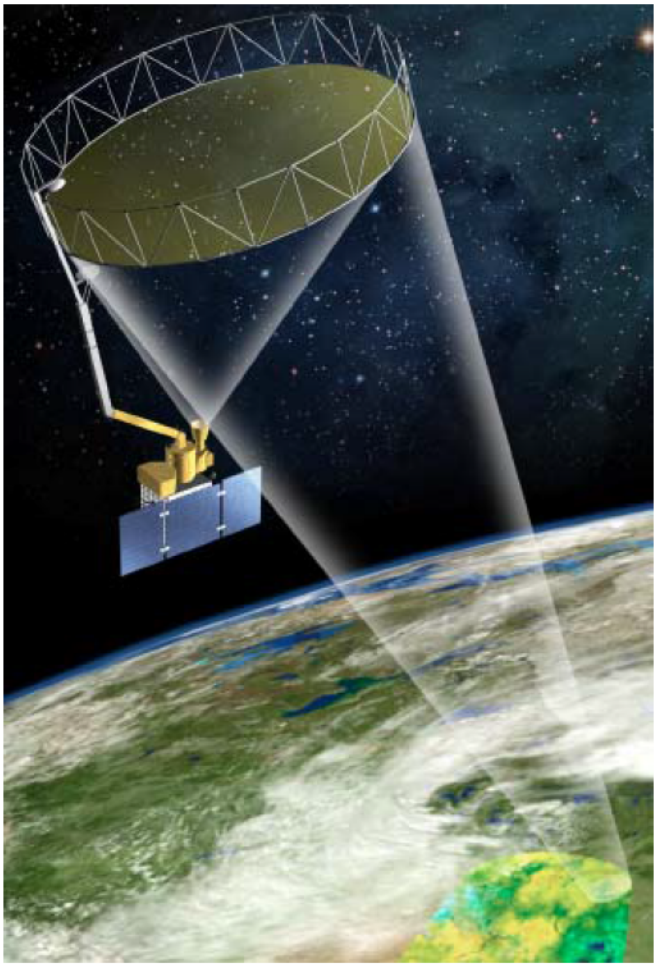

Figure 1. Artist rendition of SMAP in orbit, showing the mesh antenna, antenna spot beam, and wide swath.

Whereas the radiometer resolution is defined as the real-aperture antenna footprint, the higher resolution radar measurements are obtained by utilizing synthetic aperture radar (SAR) processing. These are common techniques, but newly applied to a scanning mesh antenna.

II. SMAP RADAR DESIGN

As with most microwave instruments, the antenna is the dominant instrument subsystem that determines both the ultimate measurement performance and governs spacecraft accommodation. In order to meet the 3-day refresh requirement at the equator, a wide measurement swath is necessary. The requirement for radiometer and radar spatial resolution at L-Band dictate that a relatively large antenna aperture must be employed. As determined by previous trade-off studies [3], the most economical approach for accomplishing the required simultaneous radiometer and radar requirements is to utilize a shared antenna/feed approach. A reflector antenna was chosen to ensure that system calibration requirements, primarily for the radiometer, are met. Large, rotating antennas have been proposed for L-Band remote sensing in the past [3]. As suggested by Fig. 1, rotating the reflector in a conical fashion about the nadir axis provides a wide swath.

A unique aspect of SMAP is the necessity for rotating the large antenna. At the nominal SMAP altitude of 685 km, the reflector must be rotated at a rate of 13.0 rpm to maintain contiguity (i.e., minimum overlap) of the measurements in the along-track direction. To obtain the required 3 km and 10 km resolution for the freeze/thaw and soil moisture products, the radar will employ pulse compression in range and Doppler discrimination in azimuth to sub-divide the antenna footprint. This is equivalent to the application of synthetic aperture radar (SAR) techniques to the conically scanning radar case [4]. Due to squint angle effects, the high-resolution products will be somewhat degraded within the 300-km region of the swath centered on the nadir track, with azimuth resolution capability decreasing over this region as the pixel location approaches the spacecraft sub-satellite track. The baseline system has both V- and H-pol channels. An additional channel measures the HV (or VH) cross-pol return.

Table 1 - SMAP radar parameters.

Antenna Key Parameters	
Beamwidth (1-way, 3 dB)	2.7°
Look Angle, Incidence Angle	35.5°, 40.0°
Peak Gain	36 dBi
Rotation Rate	13.0 rpm
Radar Key Parameters	
Transmit Carry Frequencies	Tunable from 1.22 to 1.30 GHz
Channels	HH, VV, HV (or VH)
PRF, Pulse Length	2.9 kHz, 15 µsec
Azimuth Dwell Time	42 ms
Transmit Bandwidth	1 MHz
Peak Transmit Power	500 W (at output of amplifier)
Single-look res (broadside)	250 m x 400 m
Noise Equiv. σ° (broadside)	-31 dB

The radar relative error depends on the signal-to-noise ratio (SNR) and the number of independent samples (or "looks") averaged in each measurement, as well as the relative calibration error. Looks will be obtained by averaging in both range and azimuth. The 1-MHz bandwidth will yield a ground range resolution of approximately 250 m and will result in 12 looks in range at 3 km resolution. The Doppler diversity will be maximized at a scan angle perpendicular to the platform velocity, leading to a single-look azimuth resolution of approximately 400 m. The single-look resolution will degrade as the scan angle approaches the platform velocity vector, reaching 1500 m at the inner swath edge (150 km cross-track). Table 1 provides a summary of the SMAP radar performance requirements.

Figure 2 displays a simplified block diagram of the SMAP radar functions. As the antenna rotates at a rate of 13 rpm, the SMAP radar emits H-polarized and V-polarized pulse pairs at a pulse repetition frequency (PRF) of approximately 2850 Hz (see Fig. 3.) The exact PRF varies slightly around the orbit to account for Earth oblateness. Each pulse is 15 microseconds in length, and is modulated to a linear-FM chirp of 1 MHz bandwidth. The H-pol and V-pol signals are transmitted in succession with a separation of 9 microseconds using a single high-power transmitter, and routed respectively to the H-pol and V-pol ports of the antenna by a polarization selection switch. The H-pol and V-pol transmit signals are at two different frequencies, f_H and f_V, separated by 3 MHz. This frequency separation allows the resultant echoes from each transmit polarization to be distinguished during their simultaneous reception (see Fig.'s 3 and 4).

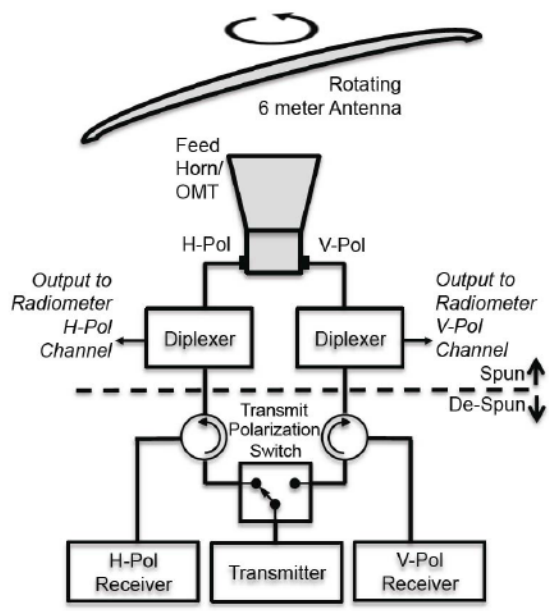

Figure 2. Simplified radar block diagram.

In essence, the SMAP radar can be thought of as two simultaneously operating dual-pol systems, one measuring HH and VH polarization, the other measuring VV and HV polarization (where the convention of the notation used here is ordered first "receive polarization" then "transmit polarization.") Upon receive, the signals from the V- and H-polarized antenna ports are routed to two identical receivers. After downconversion and sampling, each receiver applies a set of three digital filters (see Fig. 4). In the H-channel receiver, there is a 1 MHz filter centered on f_H to measure the HH co-polarized backscatter, and a filter centered on f_V to measure the HV cross-polarized backscatter. The situation is reversed in the V-channel receiver where f_V and f_H measure the VV co-polarized backscatter and VH cross-polarized backscatter respectively.

The output samples from the co-polarized and cross-polarized filtering operations are telemetered to the ground for SAR processing. In both receivers, there is also a 1 MHz "noise-only" filter in between the transmit frequencies for the purpose of measuring the thermal noise background. We note that SMAP is a relatively narrow-band radar compared to other spaceborne SARs. This is consistent with the SMAP mission's moderate spatial resolution requirements. Following a standard technique utilized in radar scatterometry, a measurement of thermal noise power is subtracted from the signal power in ground data processing. This is a necessary step to prevent biasing the backscatter measurement at low signal levels. All of the filters are designed with high out-of-band rejection to ensure suppression of RFI signals at frequencies outside the filter pass bands.

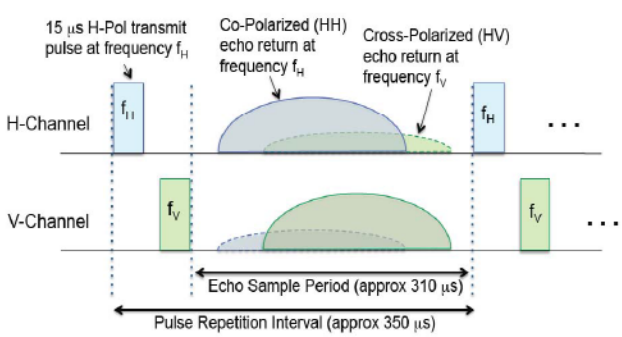

Figure 3. Radar timing.

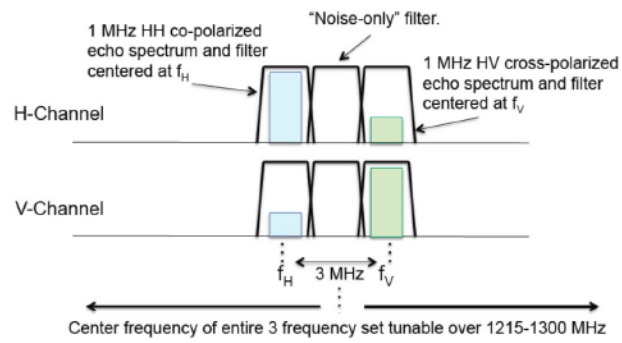

Figure 4. Radar frequencies and filtering.

A key feature of the SMAP radar design is that the transmit frequencies, along with the associated filter center frequencies, can be tuned anywhere within the 1215 MHz to 1300 MHz remote sensing allocation (Fig. 4) in steps of 1.25 MHz. Tuning to the desired frequency is accomplished by using a look-up table that is dependent on geographic location. Because of anticipated strong radio-frequency interference (RFI), this tuning capability was implemented to allow frequency adjustments in response to persistent interferers operating at a specific location, or in response to new emitters that may appear over time. Indeed, studies with current and previous L-Band systems have indicated that many emitters appear stationary in frequency, which suggests that interference might be avoided by tuning away from them. Because the SMAP radar is relatively narrow band, the operating frequency could potentially be placed in RFI-clear regions between the spectra of other emitters. Despite the capability to select spectral regions in which to operate, it is expected that there will still be significant RFI that appears in the data and will need to be mitigated by ground data processing. The subject of RFI has been extensively studied for SMAP and is treated elsewhere (e.g., see [5]).

III. Freeze/Thaw Measurements

The SMAP mission is intended to measure soil-moisture and freeze/thaw state. In this paper, particular focus is placed on freeze/thaw state. The terrestrial cryosphere comprises cold areas of the Earth's land surface where water is either permanently or seasonally frozen. This includes most regions north of 45 degrees North latitude and most areas with elevation greater than 1000 meters. Within the terrestrial cryosphere, spatial patterns and timing of landscape freeze-thaw state transitions are highly variable with measurable impacts to climate, hydrological, ecological and biogeochemical processes.

Satellite-borne microwave remote sensing has unique capabilities that allow near real-time monitoring of numerous landscape processes associated with a single

measurement of freeze/thaw state, without many of the limitations of optical-infrared sensors. The SMAP product is designed to provide the most accurate remote sensing-based characterization of landscape freeze-thaw state available at a global scale. The unique design of the SMAP L-band radar allows a combined spatial and temporal characterization of terrestrial freeze-thaw transitions previously unavailable.

The baseline SMAP product is designed to fulfill the SMAP mission freeze-thaw science requirements. The baseline product provides freeze-thaw state classification information with a multi-look spatial resolution of 3 km with temporal revisit of 2 days or better north of 45N and 3 days or better elsewhere. The data product will be global in extent, covering unmasked regions of the Earth's land mass where low temperatures are a significant constraint to vegetation productivity and terrestrial carbon exchange.

Combining SMAP freeze/thaw state assessments from AM and PM acquisitions provides unique information on regions undergoing freeze/thaw transitions on a diurnal (day/night) basis. This aspect of the product supports enhanced investigation of spring and autumn transition seasons and the associated controls on annual vegetation productivity. The radar freeze-thaw algorithm will also supply a 3 km resolution A.M. global binary freeze/thaw state flag as an intermediate output product to be utilized within the radar soil moisture processing to identify frozen land regions.

The seasonal threshold algorithm examines the time series progression of the remote sensing signature relative to signatures acquired during seasonal reference frozen and thawed states. This algorithm is well-suited for application to data with temporally sparse or variable repeat-visit observation intervals and has been applied to ERS and JERS Synthetic Aperture Radar (SAR) imagery [1][7][8][9]. A seasonal scale factor Δ(t) may be defined for an observation acquired at time t as:

$$\Delta(t) = \frac{\sigma(t) - \sigma_{fr}}{\sigma_{th} - \sigma_{fr}} \qquad (1)$$

where $\sigma(t)$ is the measurement acquired at time t, for which a freeze/thaw classification is sought, and σ_{fr} and σ_{th} are backscatter measurements corresponding to the frozen and thawed reference states, respectively. In situations where only a single reference state is available, for example σ_{fr}, $\Delta(t)$ may be defined as a difference:

$$\Delta(t) = \sigma(t) - \sigma_{fr} \qquad (2)$$

A threshold level T is then defined such that:

$$\Delta(t) > T$$
$$\Delta(t) \leq T$$

defines the thawed and frozen landscape states, respectively. This series of algorithms will be run on a cell-by-cell basis for unmasked portions of the domain. The output will be a dimensionless binary state variable designating either frozen or thawed condition for each unmasked grid cell. Whereas Equation (1) accounts for differences in the dynamic range of the remote sensing response to freeze/thaw transitions driven by variations in land cover, Equation (2) does not scale $\Delta(t)$ to account for the dynamic range in the seasonal response. The selection of parameter T may be optimized for various land cover conditions and sensor configurations. In situations where the wintertime microwave signature is not dominated by the snow pack volume, for example for radar measurements at lower frequencies (*e.g.* L-band) and where shallow dry snowpacks are common, $\sigma_{fr} < \sigma_{th}$ and $\Delta(t) > T$ defines the thawed state.

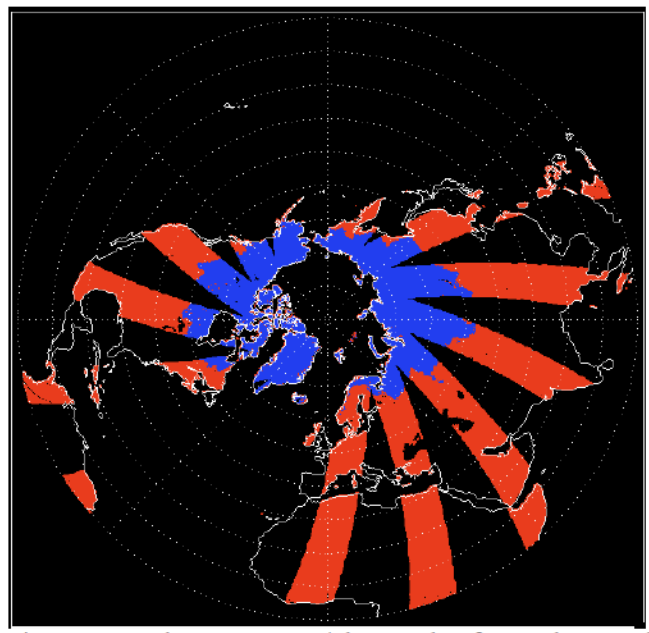

Figure 5. Sample SMAP Freeze/Thaw product for one day's worth of AM passes (blue = frozen, red = thawed).

Refinement and testing of SMAP freeze-thaw algorithms will involve utilizing satellite L-band SAR (e.g., JERS-1 SAR, ALOS PALSAR, and Aquarius) and radar backscatter models to assess the simulated SMAP radar backscatter response over a variety of environmental, terrain and land cover conditions in order to assess these error sources. Primary sources of error and uncertainty in the freeze/thaw product stems from: (1) radiometric errors due to resolution and sensor viewing geometry (azimuth), (2) geometric errors due to layover and shadowing (slope/aspect), (3) within-season radar backscatter variability not accounted for by the implementation of the constant frozen and thawed reference states employed within the baseline algorithm, and (4) variations in landcover with respect to spatial heterogeneity. Some additional sources are associated with

relatively dry landscapes that contain small amounts of water such that changes in freeze/thaw state result in minimal change in backscatter. Also, large precipitation events that significantly wet the land surface such that the additional surface water induces a pronounced backscatter may induce an error in the classified freeze/thaw state. Integrating JERS-1 and PALSAR data sets within the SMAP Science Data System (SDS) Testbed will support investigation of system level parameters (e.g. system noise, viewing geometry, and associated topographic effects) in the error and uncertainty assessment.

The classification accuracy of freeze-thaw state was simulated using the expected SMAP system noise vs. the difference in backscatter between the thawed and frozen states (Figure 3). A step size of at least 1.5 dB will meet the classification accuracy of 80%, calculated on an annual basis.

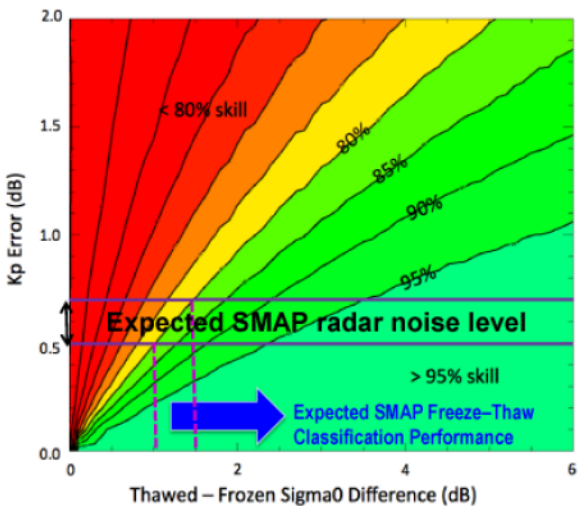

Figure 3. Simulation of classification accuracy versus radar noise and freeze/thaw state step size in backscatter. The required accuracy or skill is 80%.

Acknowledgment

The research described in this paper was carried out at the Jet Propulsion Laboratory, California Institute of Technology, under a contract with the National Aeronautics and Space Administration.

References

[1] D. Entekhabi, E. Njoku, P. Houser, M. Spencer, T. Doiron, J. Smith, R. Girard, S. Belair, W. Crow, T. Jackson, Y. Kerr, J. Kimball, R. Koster, K. McDonald, P. O'Neill, T. Pultz, S. Running, J.C. Shi, E. Wood, J. vanZyl, "The Hydrosphere State (HYDROS) Mission: An Earth System Pathfinder for Global Mapping of Soil Moisture and Land Freeze/Thaw," *IEEE Transactions on GeoScience and Remote Sensing*, Vol. 42, No. 10, October 2004, pp. 2184-2195.

[2] M. Spencer, K. Wheeler, C. White, R. West, J. Piepmeier, D. Hudson, J. Medeiros, "The Soil Moisture Active Passive (SMAP) Mission L-Band Radar/Radiometer Instrument," *Proceedings of IGARSS, Honolulu, HI, July*, 2010.

[3] E. Njoku, W. Wilson, S. Yueh, R. Freeland, R. Helms, W. Edelstein, G. Sadowy, D. Farra, R. West, K. Oxnevad, T. Campbell, W. Lawrence, Y. Rahmat-Samii, H. Feingold, G. Didinsky, J. Rauwolf, M. Thompson, G. Konicke, "Spaceborne Microwave Instrument for High Resolution Remote Sensing of the Earth Surface Using a Large-Aperture Mesh Antenna," NASA/JPL Publication 01-09, September, 2001.

[4] M. Spencer, W. Tsai, D. Long, "High-Resolution Measurements With a Spaceborne Pencil-Beam Scatterometer Using Combined Range/Doppler Discrimination Techniques," *IEEE Transactions in Geoscience and Remote Sensing*, Vol. 41, No. 3, March 2003, pp. 567-581.

[5] J. Belz, B. Huneycutt, M. Spencer, "A Study of Radio Frequency Interference in the Space-to-Earth Exploration allocation at L-Band," *Proc. IEEE Aerospace Conf.*, Big Sky, Montana, March, 2011.

[6] J. Kimball, K. McDonald, S. Frolking and S. Running, "Radar remote sensing of the spring thaw transition across a boreal landscape." Remote Sensing of Environment 89(2), 163-175, 2004.

[7] E. Rignot, and J. Way, "Monitoring freeze-thaw cycles along north-south Alaskan transects using ERS-1 SAR," *Remote Sensing of Environment*, 49, 131-137, 1994.

[8] J. Way, R. Zimmermann, E. Rignot, K. McDonald and R. Oren "Winter and Spring Thaw as Observed with Imaging Radar at BOREAS," *Journal of Geophysical Research,* 102(D24), 29673-29684, 1997.

[9] J. Gamon, K. Huemmrich, J. Chen, D. Fuentes, F. Hall, J. Kimball, S. Goetz, J. Gu, K. McDonald, J. Miller, M. Moghaddam, D. Peddle, A. Rahman, J.-L. Roujean, E. Smith, C. Walthall, and P. Zarco-Tejada, "Remote sensing in BOREAS: Lessons learned." *Remote Sensing of Environment* 89(2), 139-162, 2004.